ISSN: 0067-2904

Effect of Atmospheric Mixing on Spectral Reflectivity in Sentinel Images of Baghdad Province

Eman S. Hassan[1], Ahmed F. Hassoon[1], Ebtesam F. Khanjer[2]
[1]*Atmospheric Department, College of Science, Mustansiriyah University, Baghdad, Iraq*
[2]*GIS and RS Department, College of Science, University of Baghdad, Baghdad, Iraq*

Received: 10/4/2023 Accepted: 13/8/2023 Published: 30/9/2024

Abstract

The lowest layer of the atmosphere is called the atmospheric mixed layer, characterized by small-scale, irregular air motions defined by winds that change in speed and direction. Aerosol radiative effects impact the atmospheric boundary layer (ABL), which holds most aerosols in the lower atmosphere. Aerosol absorption and scattering both lower the quantity of solar energy that reaches the ground, which has an impact on the spectral signature of the land coverings. In this study, 51 locations in downtown Baghdad were chosen for four different types of land cover (water bodies, farms, open areas, and residential areas) for Sentinel 2 satellite imagery, and the time the pictures were taken was 8:00 am (22 March, 22 June, 20 September, and 22 December) 2021. Their spectral reflectance was calculated at the NIR band using a mathematical equation in the ArcGIS program for Sentinel 2 satellite images that had been processed and analyzed. Also, atmospheric boundary layer height and solar radiation values were downloaded for the same date as the satellite images and compared with the spectral reflectivity values of the land covers(agriculture area, residential area, open area, and river) and knowing the effect of the mixing layer and solar radiation on the spectral reflectance values. The highest value of spectral reflectivity, mixing layer height, and solar radiation was in June at (0.065, 1965.524629, and 897.7088) respectively. The spectral reflectivity of plants at near-infrared (NIR) was higher than the rest of the earth's features because plants reflect near-infrared radiation and absorb the red and blue parts of the spectrum.

Keywords: Reflectivity, atmospheric boundary layer, Sentinel 2 satellite, Baghdad city, GIS.

تأثير الخلط الجوي على الانعكاسية الطيفية في صور القمر الصناعي سينتينل لمحافظة بغداد

ايمان سعد حسن[1], احمد فتاح حسون[1], ابتسام فاضل خنجر[2]
[1]قسم علوم الجو, كلية العلوم, الجامعة المستنصرية, بغداد, العراق
[2]قسم التحسس النائي ونظم المعلومات الجغرافية, كلية العلوم, جامعة بغداد, بغداد, العراق

الخلاصة

تسمى الطبقة الدنيا من الغلاف الجوي طبقة الغلاف الجوي المختلطة ، وتتميز بحركات هواء غير منتظمة صغيرة الحجم تحددها الرياح التي تتغير في السرعة والاتجاه. تؤثر التأثيرات الإشعاعية للهباء على طبقة الحدود الجوية (ABL) ، التي تحتوي على غالبية الهباء الجوي في الغلاف الجوي السفلي. يقلل امتصاص الهباء الجوي وتناثره من كمية الطاقة الشمسية التي تصل إلى الأرض ، مما يؤثر على البصمة

*Email: emansaadhassn1991@gmail.com

الطيفية للأغطية الأرضية. في هذه الدراسة ، تم اختيار 51 موقعًا في وسط مدينة بغداد لأربعة أنواع مختلفة من الغطاء الأرضي (المسطحات المائية والمزارع والمناطق المفتوحة والمناطق السكنية) لصور القمر الصناعي Sentinel 2 ، وكان وقت التقاط الصور الساعة 8:00 صباحًا (22 مارس و 22 يونيو و 20 سبتمبر و 22 ديسمبر) 2021. تم حساب انعكاسها الطيفي في نطاق NIR باستخدام معادلة رياضية في برنامج ArcGISلصور القمر الصناعي Sentinel 2 التي تمت معالجتها وتحليلها. أيضًا ، تم تنزيل ارتفاع طبقة الحدود الجوية وقيم الإشعاع الشمسي لنفس تاريخ صور القمر الصناعي ومقارنتها بقيم الانعكاسية الطيفية لأغطية الأرض (منطقة الزراعة ، المنطقة السكنية ، المنطقة المفتوحة ، النهر) ومعرفة تأثير طبقة الخلط والإشعاع الشمسي على قيم الانعكاس الطيفي. كانت أعلى قيمة للانعكاسية الطيفية وارتفاع طبقة الخلط والإشعاع الشمسي لشهر يونيو بواقع (0.065 و 1965.524629 و 897.7088) على التوالي. كانت الانعكاسية الطيفية للنباتات في الأشعة تحت الحمراء القريبة (NIR) أعلى من بقية ميزات الأرض لأن النباتات تعكس الأشعة القريبة من الأشعة تحت الحمراء وتمتص الأجزاء الحمراء والزرقاء من الطيف

.

1. Introduction

The convective boundary layer or the mixing layer is the turbulent layer of the atmosphere adjacent to the earth's surface that occurs during the daytime over a short timescale (hours). After sunrise, the surface absorbs solar radiation, and the air above the surface becomes unstable; turbulence and the atmospheric boundary layer develop. Atmospheric turbulence influences the mixing of gases and particles, where turbulent flows can impact aerosol and particles' evolution and spatial distribution in the atmosphere[1]. The transition zone is an essential feature of the mixing layer, characterized by considerable variability in pollutants and ambient temperature and humidity values between the well-mixed boundary layer and the stable free troposphere[2]. In meteorological, climate, and air quality models, mixing layer height (MLH) is a crucial length scale to calculate turbulence mixing, vertical diffusion, convective transport, and atmospheric pollutant deposition[3]. The downward and upward radiance detected above the earth's atmosphere is impacted by the scattering and absorption of solar radiation by atmospheric aerosol and molecules. The wavelength of the radiation has a significant impact on air scattering and absorption. Compared to long wavelengths, scattering is typically substantially stronger for shorter wavelengths. The classification of surface features and the remote sensing of the vegetation index are both impacted by air scattering because of its considerable wavelength dependency [4].

A reduction in the power of solar radiation owing to absorption, scattering, and reflection in the atmosphere can be used to explain the atmospheric effect caused by molecule and aerosol scattering and absorption of solar radiation. Diffusion widens the radiation's angular distribution, which causes it to interact with the surface in a variety of directions (instead of the solar beam's direction) so that the reflection coefficient of the surface that corresponds to this radiation is not the same as the reflection coefficient of the direct solar beam [5]. A shift in solar radiation's spectral composition brought on by more intense absorption or scattering of certain wavelengths. Furthermore, scattering leads to radiation diffusion, bringing photons reflected from the region outside the field of view into the field of view[6]. Without being reflected by the surface, light from the direct solar beam enters the field of view and is scattered in the atmosphere. This element makes the picture brighter. For dark surfaces, its impact is particularly substantial [7]. It is simple to differentiate vegetation from other land cover types thanks to its characteristic spectral signature. The reflectance in the near-infrared (NIR) region is significantly higher than in the visible range due to the cellular network that makes up the leaf structure. Due to this, vegetation can be recognized by its strong NIR reflectance but generally low visible reflectance. When silt, plankton, or chlorophyll are in the water, this reflectivity increases in the visual range. Clean water typically has a low reflectance. Water appears completely black and has the maximum reflection at the blue

section of visible wavelengths. It also has the highest near-infrared (NIR) absorption[8]. The factors that affect a soil's reflectivity include its moisture content, organic matter content, particle size distribution, iron oxide content, minerals in the soil, and soil structure. Wet soil has high reflectivity compared to dry soil. With increasing wavelength, reflectance gets more robust in the SWIR band (short wave infrared) and weaker in the red band. The diversity of building materials used in metropolitan settings causes spectral reflectivity, a composite of reflections from two or more classes, to vary. Red radiation absorption is decreasing along with spectral reflectivity in the infrared range, while green reflectivity is increasing. The spectra frequently overlap. Given that the two have comparable spectral reflectivities and since rocks are a crucial part of buildings, there is frequently overlap between the spectral reflectivity of urbanization and the spectral reflectivity of rocky soil in urban areas with surrounding vegetation [9]. Z. M. Abbood and O. T. Al-Taai computed the solar radiation absorption and emission by clouds, aerosols, and methane gas in 2018. The findings revealed that the most robust inverse correlation coefficient at 0:00 am was -0.9, and the highest positive correlation value with CH4 was 0.6. where there is a strong association, which was then followed by clouds and aerosols[10]. The spectral reflectivity of the various elements of Iraq's lands, including various kinds of green plants, soil, water, metal, and concrete roofs, were studied in 1988 by N. H. Al-Mafarji and Q. A. Abdullah. Notwithstanding the differences in their locations in Iraq, the spectral reflectance curves were found in four bands covering the range from (0.5 - 1.1) microns after being separated into (37) different groups based on their similar spectral behavior and close quality [11]. The study aims to know the effect of atmospheric mixing conditions resulting from the vertical convective movement of the atmosphere and the horizontal mechanical movement on the spectral signature change of the surface components of Baghdad city (agriculture area, open area, river, and residential area) in the bands of the Sentinel satellite images, which consists of 13 spectral bands.

2. Data and Location

2-1 Study area

Baghdad is the capital of Iraq, with the highest population in the country, with 8.4 million people in 2016. It has 14 administrative units, eight in Al-Rasafa (east of the Tigris River) and six in Al-Karkh. The study area is between longitudes 44.189 and 44.576 degrees east and latitudes 33.452 and 33.184 degrees north. The study area has high-temperature extremes, little precipitation, low relative humidity, and high sun brightness[12]. Figure 1 shows the location of the study area [12].

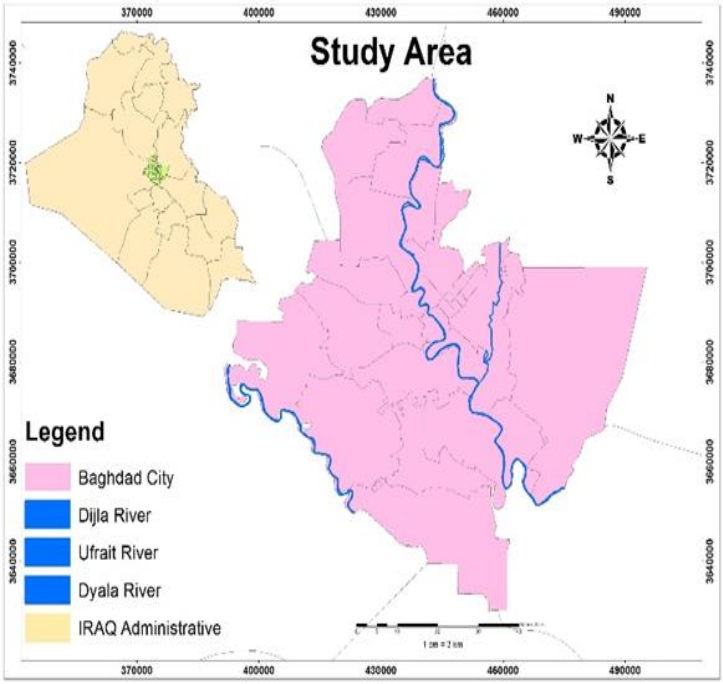

Figure 1: The location of the study area, Baghdad Capital, Iraq.

2-2 Data Source and Processing

Sentinel2 satellite data downloaded from the website (https://scihub.copernicus.eu) for the months (March, June, September, and December) of 2021 and are high-resolution images consisting of 13 spectral bands, providing visual information ranging from the visible to Near- and mid-infrared bands with spatial resolution ranging from 10 m to 60 m. Then the following operations were performed (mosaic images, cropping of the study area, processing of satellite images, conversion DN to reflectance). Boundary layer values were downloaded from ERA5 (European Environment Agency) and are the fifth generation of ECMWF (European Centre for Medium-Range Weather Forecasts) atmospheric reanalysis of the global climate covering the period from January 1950 to the present on the exact dates of the satellite images. Table 1 describes the information on sentinel-2 satellite bands [13]; the range used in this study are (B8).

Table 1: shows the information on sentinel-2 satellite bands.

Band number	Descriptions	Resolution(m)	Wavelength(nm)
B1	Coastal aerosol	60	443
B2	Blue	10	490
B3	Green	10	560
B4	RED	10	665
B5	Vegetation RED edge	20	705
B6	Vegetation RED edge	20	740
B7	Vegetation RED edge	20	783
B8	Near-infrared (NIR)	10	842
B8a	Vegetation RED edge	20	865
B9	Water vapor	60	945
B10	SWIR-CIRRUS	60	1380
B11	SWIR	20	1910

3. Methodology

3.1 Stages of generation Convective Boundary Layer

The lower troposphere's convective boundary layer (CBL) is the region most directly impacted by solar heating of the earth's surface [14]. This layer stretches from the earth's surface to a capping inversion, which usually forms by mid-afternoon over land at a height of 1-2 km. The two sub-layers are the mixed layer, which makes up 35–80% of the CBL depth, and the surface layer, which makes up 5%–10% of the CBL depth. Because of the substantial buoyancy produced by convective turbulent mixing, the mixed layer, which constitutes most CBL, has a relatively fairly constant distribution of variables, including potential temperature, wind speed, moisture, and pollutant concentration [15]. Because of the solid overnight stable inversion capping, the mixed layer is shallow in the morning and gradually gets deeper. In the second phase, the thermals penetrate quickly upward because, by the late morning, the cool nocturnal air has warmed to a temperature that is close to that of the residual layer, allowing the top of the mixed layer to climb at speeds of up to 1 km every 15 minutes. The growth rate of the mixed layer rapidly declines as the thermals encounter resistance to vertical motion when they reach the capping inversion at the top of the residual layer. This third stage, which lasts most of the afternoon. The mixing-driven turbulence caused by buoyancy decays at sunset, and the CBL collapses. Convective turbulence is mainly caused by buoyancy created by ground surface heating in the mixed layer. The updrafts and downdrafts of boundary layer convection are the principal means by which the atmosphere transports heat, momentum, moisture, and pollutants between the Earth's surface and the atmosphere. Determining the dynamics of multiple mesoscale events, numerical weather prediction and global climate modeling depend on boundary layer convection[16]. Figure 2 shows the convective boundary layer.

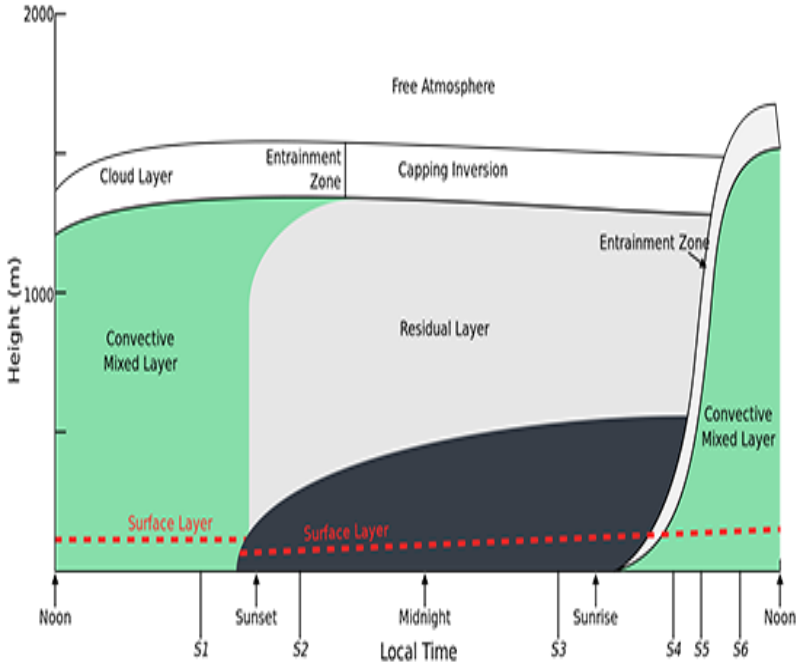

Figure 2: The convective boundary layer.

3.2 spectral reflectivity

The ratio of reflected energy to incident energy as a function of wavelength is known as spectral reflectance. On the land's surface, many materials have different spectral reflectance characteristics. For a particular feature of the topography on the Earth's surface, the spectral

reflectance depends on the wavelength and has different values at different wavelengths [17]. Digital Number is the pixel values' distinctive or common names (DN). Often, it refers to pixel values that have not yet been calibrated into physically meaningful units. Because they are mathematical values or representations of spectral data without physical magnitudes, it is not advised to use them directly to calculate environmental information; therefore, we must convert units of the immaterial to physical units to obtain a better illustration of the spectral response of the objects. Reflectance is better than DN values since it is a continuous target characteristic, whereas DN values change with radio resolution [18].

The following equation was used to convert the digital number (DN) into a radiance [19]:

$$radiance = ((pixelvaluebandx * cos\ (incidenceangle) * solarirradiancebandx)/(\pi * d2))/10000 \quad (1)$$

Where d2 is 1.0/U.

Then we used this equation to convert radiance to reflectance:

$$Reflectance = (Radiance \times \pi \times d\text{^}2) / (ESUN \times cos(\theta)) \quad (2)$$

Reflectance is the surface reflectance value.

Radiance is the top of atmosphere radiance value

π is the mathematical constant pi (3.14159...).

d is the Earth-Sun distance in astronomical units (AU) in the Sentinel-2 metadata.

ESUN is the extraterrestrial solar irradiance value for the Sentinel-2 spectral band, found in the Sentinel-2 user handbook.

θ is the solar zenith angle, also found in the Sentinel-2 metadata.

4. Result and Discussion

The spectral reflectivity values for the different land covers (agriculture area, river, residential area, and open area) were calculated using a mathematical equation in the ArcGIS program and knowing the effect of the atmospheric mixing layer and solar radiation on the spectral reflectivity. Initially, we process satellite images:

4.1 Images Processing

A Mosaic is a process of overlapping or merging two or more images to form one mixed image file so that the mixed image does not have occlusion borders in the transition region while preserving the overall appearance of the original images. In ArcGIS Version 10.2, through this tool, a single raster dataset from multiple raster datasets. It can be created by mosaicking them with each other. This tool is used to include all parts of the province of Baghdad, using ground markers in the areas of the installation between neighboring images.

In GIS, a clip tool overlays a polygon on one or more target features (layers) and extracts from the target feature (or features) only the target feature data within the area outlined by the clip polygon. In other words, the boundaries of the second polygon are imposed on the first polygon. Thus the image clipping increases the accuracy of the work, Figure 3.

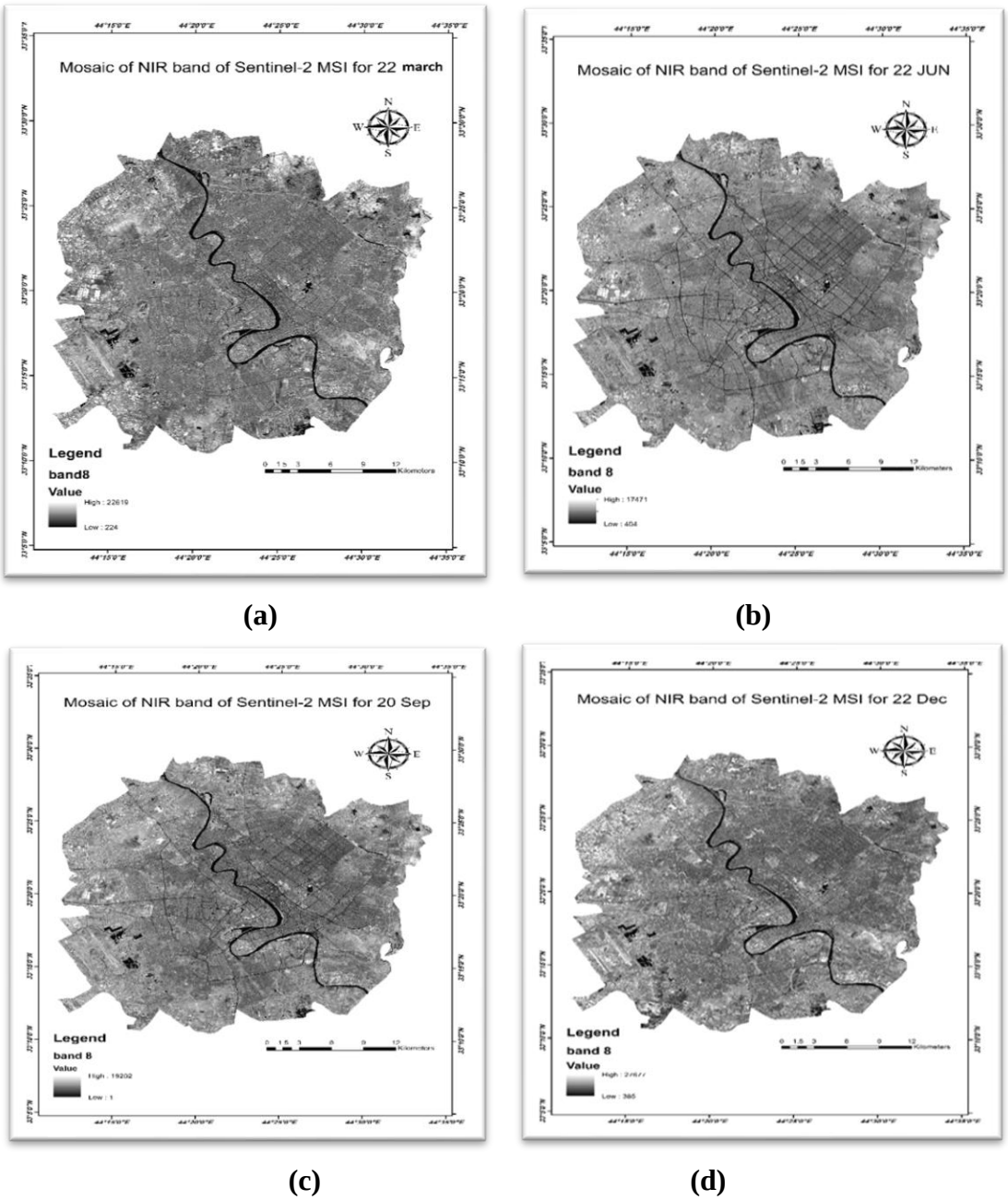

Figure 3: The mosaic image and clip bands of sentinel images for the NIR band in (a) March, (b) June, (c) September, and (d) December.

4.2 Convert DN (digital number) to Reflectance

The general term for pixel values, or their distinguished name, is Digital Number (DN). It is not recommended to use them directly to calculate environmental information because they are mathematical values or representations of spectral data without physical magnitudes, which is because it is converted units of the immaterial to physical units to get a better representation of the spectral response of the objects. Reflectance is superior to DN values because the former is a constant property of the target, whereas the latter varies with radio resolution. The most important surface features are color, structure, and surface texture; these differences make it possible to identify different earth surface features or materials by analyzing their spectral reflectance patterns or signatures, Figure 4.

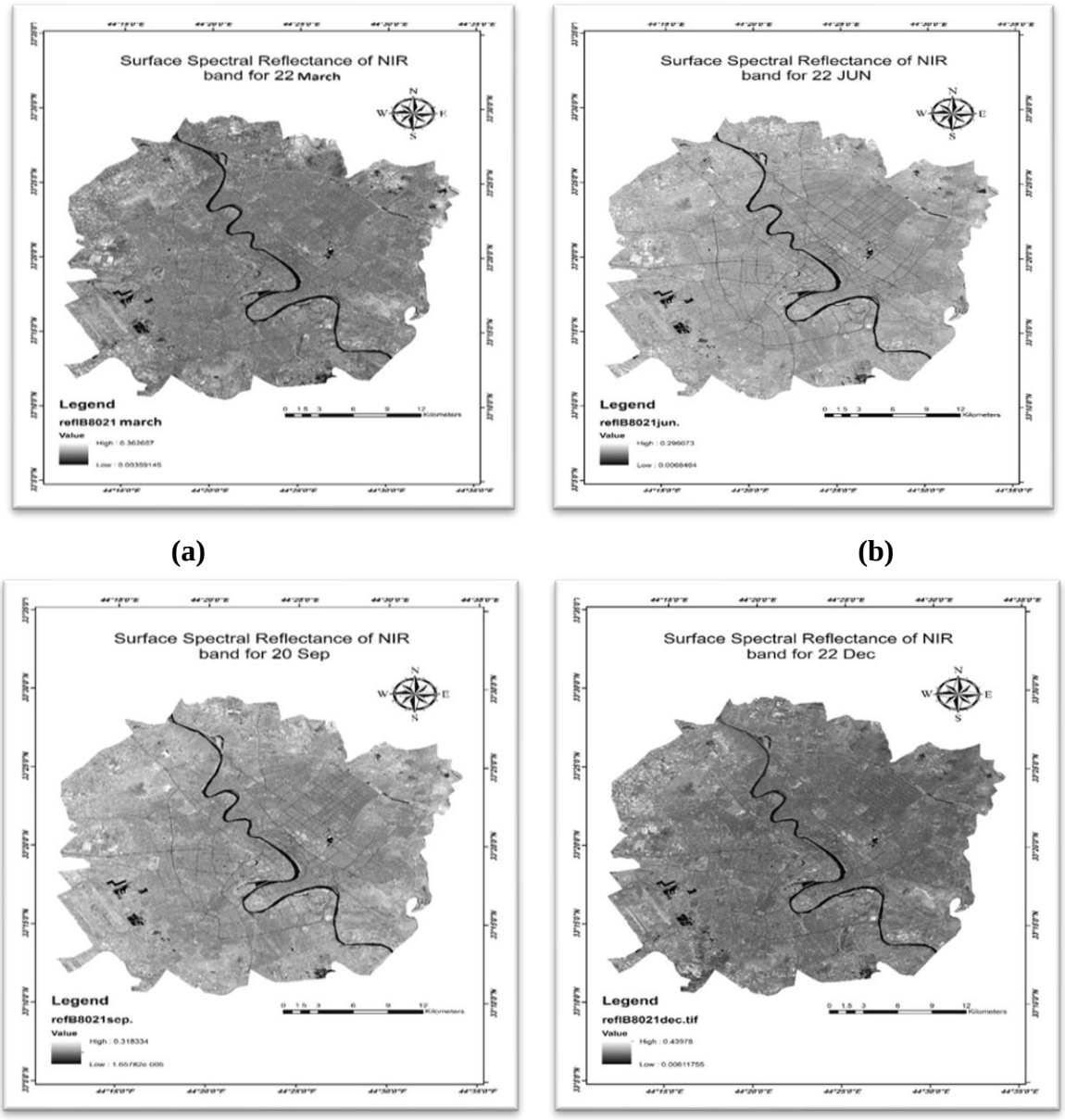

Figure 4: Converting of DN to the reflectance of sentinel image in (a) March, (b) June, (c) September, and (d) December.

4.3 Spectral Reflectivity with Land Covers

After calculating the spectral reflectivity values of the different land covers (agriculture, residential, rivers, and open area) at the near-infrared band (NIR), a relationship was made between the spectral reflectivity and the ground features, that shows the difference in the spectral reflectivity values of these ground covers at different times of the year. The values of the spectral reflectivity of the different land covers with the seasons of the year are variable as a result of the difference in the amount of solar radiation reaching the surface of the earth and the change in the height of the mixing layer which affects on the solar radiation reaching the surface of the earth, and the highest value of the spectral reflectivity was in the summer season, Figure 5.

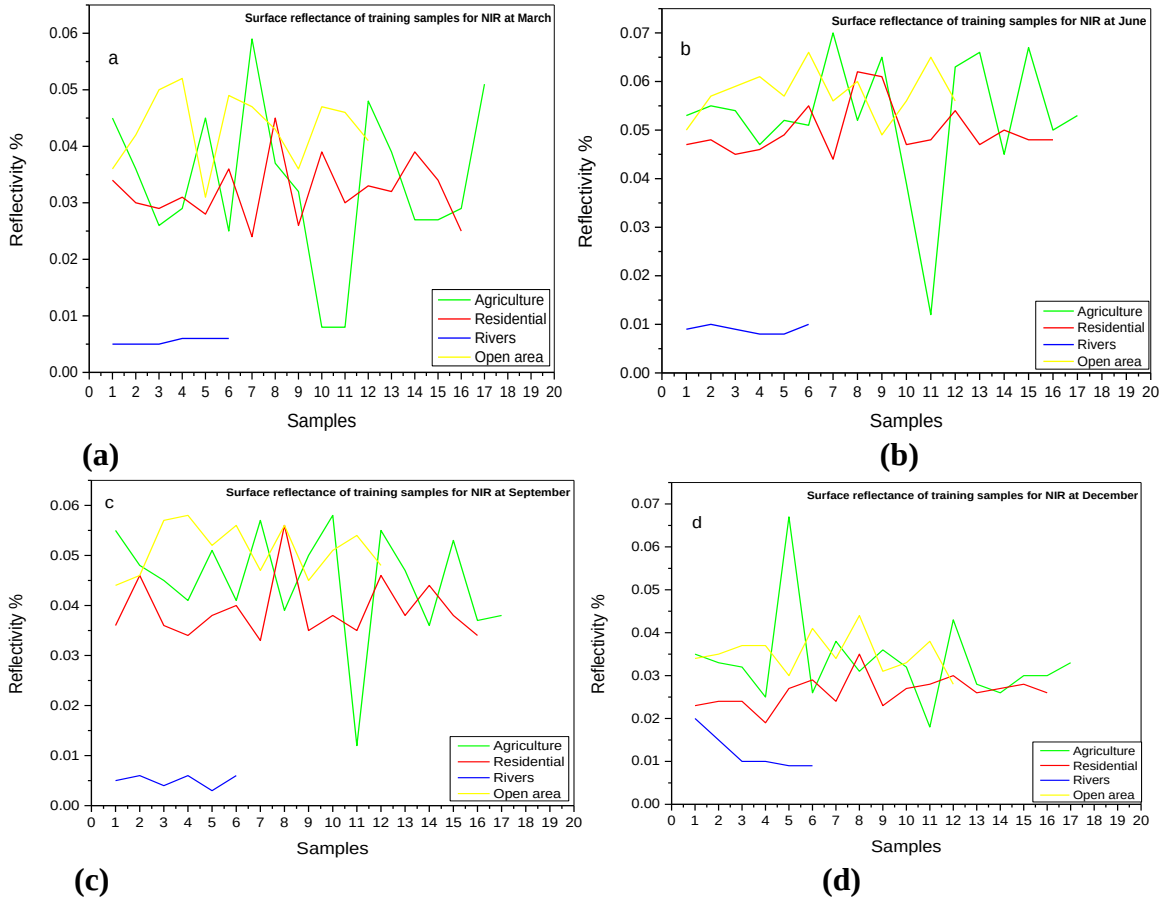

Figure 5: The relationship between reflectivity and land covers for the NIR band in (a) March, (b) June, (d) September, and (d) December.

Download the mixing layer height (MLH) values for the exact date and time of Sentinel 2 satellite images and make a table for them to compare them and find out the effect of the mixing layer height on the spectral reflectivity.

Table 2: Spectral reflectivity at NIR band (RE-8) and mixing layer height values in (March, June, September, and December).

	March		**June**		**September**		**December**	
region	**MLH**	**RE-8**	**MLH**	**RE-8**	**MLH**	**RE-8**	**MLH**	**RE-8**
agriculture	1145.649568	0.032	1122.920448	0.065	1378.40841	0.05	420.8482022	0.036
residential	1890.87551	0.034	1677.140444	0.047	1542.799144	0.036	379.9086737	0.023
Open area	1190.158879	0.052	840.4105887	0.061	1263.768693	0.058	376.5196399	0.037
river	1741.848397	0.005	1965.524629	0.01	1474.295474	0.006	375.7062718	0.009

Download the solar radiation (SR) values for the exact date and time of Sentinel 2 satellite images and make a table for them to compare them and find out the effect of solar radiation on spectral reflectivity.

Table 3: Spectral reflectivity at NIR band (RE-8) and solar radiation values in (March, June, September, and December).

	March		**June**		**September**		**December**	
region	**SR**	**RE-8**	**SR**	**RE-8**	**SR**	**RE-8**	**SR**	**RE-8**
agriculture	736.5097	0.032	889.0794	0.065	778.3354	0.05	485.1228	0.036
residential	774.9444	0.034	897.7088	0.047	776.2774	0.036	477.4873	0.023
Open area	749.255	0.052	889.8512	0.061	776.3242	0.058	479.4751	0.037
river	768.3964	0.005	896.5746	0.001	781.551	0.006	486.5493	0.009

5. Conclusions

The spectral reflectivity values of plants at the near-infrared (NIR) it is higher in the summer solstice (22 JUN) because the plant is at the peak of its growth and maturity. While at the winter solstice (21 DEC) and the spring equinox (21 MAR), the spectral reflectivity values of plants are low due to the decrease in temperature in winter, which affects plant growth and leaf plants' fall in the autumn season. The spectral reflectivity of plants in the autumn equinox (23 SEP) is higher than the winter solstice and spring equinox because it is the beginning of the autumn season, and the leaves of plants have not fallen yet. While the spectral reflectivity values of water at near-infrared rays (NIR) are almost close at all seasonal inversions because most of the radiation falling on water bodies is absorbed or transmitted by those waters, while a small part of it is reflected. Water absorbs most of the infrared radiation, which makes the contrast between it and other surface materials very large, especially within the visible images in the infrared range, and the peak of the reflection of water is at the visible rays. Water bodies can be determined using the wavelengths of visible rays due to the reflection caused by the interaction of incoming rays with the water's surface.

The spectral reflectivity of the open areas at the near-infrared had its highest values in the summer solstice and the autumn equinox, which means that these areas in this period are dry (the soil water content is low, and the soil surface is rough). Spectral reflectance in residential areas is a combination of reflections from two or more classes rather than the spectral reflectance of a single pixel. Because they are groups of land cover types with distinctive and diverse spectral characteristics. We note that the spectral reflectivity of this land feature in the near-infrared rays (NIR) is higher at the summer solstice because these areas also contain some plants at the peak of their growth and maturity before summer's entry. From the tables of spectral reflectivity with the amount of surface solar radiation, we note that the relationship between them is direct, as the increase in the amount of solar radiation corresponds to an increase in the value of surface reflectivity. The amount of solar radiation in the summer is more significant than in the winter, spring, and autumn, with higher spectral reflectivity values in the summer than in the rest seasons.

The atmospheric boundary layer height at 8:00 am in the autumn and spring seasons is higher than that of the summer season, and therefore the spectral reflectivity values of the different land covers are less than that of the summer season, which means that the mixing layer affects the spectral reflectivity of the land covers. The values of mixing layer height over the residential areas and water are higher than the rest of the land covers due to the high relative humidity at the river, which caused an increase in thermal connection with the air over it, thus increasing the thickness or high of the mixing layer. In contrast, for the residential areas, the height of the mixing layer depends on the pollutants percentage in these areas and the number of trees within the residential areas and, thus, the effect on the air in contact with them.

AKNOLOGEMENT

Thanks and praise to God Almighty first for the blessing of patience and ability to accomplish the work.

I extend my sincere thanks and great gratitude to the honorable Professor Dr. Ahmed Fattah Hasson and Professor Dr. Ebtisam Fadel Khanjar for what they provided me with helpful useful knowledge, distinguished giving, and continuous guidance, and for their continuous effort, advice, and guidance from the beginning of the research stage, and thanks also to the College of Science and the Department of Atmospheric Sciences at Mustansiriyah University for their excellent provision and facilitation of services to students and their assistance in all

matters that would give them a comfortable space to study and seek knowledge in safety and order.

References:

[1] D. Summa, P. Di Girolamo, D. Stelitano, and M. Cacciani, "Characterization of the planetary boundary layer height and structure by Raman lidar: comparison of different approaches," *Atmos. Meas. Tech.*, vol. 6, no. 12, pp. 3515–3525, 2013.

[2] K. C. Wang, R. E. Dickinson, M. Wild, and S. Liang, "Atmospheric impacts on climatic variability of surface incident solar radiation," *Atmos. Chem. Phys.*, vol. 12, no. 20, pp. 9581–9592, 2012.

[3] J. Quan *et al.*, "Evolution of planetary boundary layer under different weather conditions, and its impact on aerosol concentrations," *Particuology*, vol. 11, no. 1, pp. 34–40, 2013.

[4] Y. J. Kaufman and R. S. Fraser, "The effect of finite field size on classification and atmospheric correction," 1981.

[5] T. Lee and Y. J. Kaufman, "The effect of surface non-Lambertianity on remote sensing of ground reflectance and vegetation index," *IEEE Trans. Geosci. Remote Sens*, vol. 24, pp. 699–708, 1986.

[6] Y. J. Kaufman, "Solution of the equation of radiative transfer for remote sensing over nonuniform surface reflectivity," *J. Geophys. Res. Ocean.*, vol. 87, no. C6, pp. 4137–4147, 1982.

[7] R. S. Fraser and Y. J. Kaufman, "The relative importance of aerosol scattering and absorption in remote sensing," *IEEE Trans. Geosci. Remote Sens.*, no. 5, pp. 625–633, 1985.

[8] E. F. Khanjer, M. A. Yosif, and M. A. Sultan, "Air quality over Baghdad City using ground and aircraft measurements," *Iraqi J. Sci.*, vol. 56, no. 1C, pp. 845–893, 2015.

[9] Z. A. Abdullah and H. M. Abduljabbar, "The water bodies in the Southern East of Iraq before and after 2018," in *AIP Conference Proceedings*, 2020, vol. 2307, no. 1, p. 20032.

[10] Z. M. Abbood and O. T. Al-Taai, "Study of Absorbance and Emissivity Solar Radiation by Clouds, Aerosols and Some Atmospheric Gases," *J. Appl. Adv. Res.*, no. October 2019, pp. 128–134, 2018, doi: 10.21839/jaar.2018.v3i5.222.

[11] N. H. Al-Mafarji and Q. A. Abdullah, "A study of the spectral reflectivity of the country's lands for the purposes of camouflage and remote sensing," Mustansiriyah University, 1988.

[12] H. B. Mohammed and S. M. Abdullah, "Using remote sensing data and GIS to evaluate air pollution and their relationship with land cover and land use in Baghdad City," 2010.

[13] J. Delegido, J. Verrelst, L. Alonso, and J. Moreno, "Evaluation of sentinel-2 red-edge bands for empirical estimation of green LAI and chlorophyll content," *Sensors*, vol. 11, no. 7, pp. 7063–7081, 2011.

[14] S. Liu and X. Z. Liang, "Observed diurnal cycle climatology of planetary boundary layer height," *J. Clim.*, vol. 23, no. 21, pp. 5790–5809, 2010, doi: 10.1175/2010JCLI3552.1.

[15] A. A. M. Holtslag and B. A. Boville, "Local versus nonlocal boundary-layer diffusion in a global climate model," *J. Clim.*, vol. 6, no. 10, pp. 1825–1842, 1993.

[16] S.-Y. Hong and H.-L. Pan, "Nonlocal boundary layer vertical diffusion in a medium-range forecast model," *Mon. Weather Rev.*, vol. 124, no. 10, pp. 2322–2339, 1996.

[17] D. E. Bowker, *Spectral reflectances of natural targets for use in remote sensing studies*, vol. 1139. NASA, 1985.

[18] B. C. Hadley, M. Garcia-Quijano, J. R. Jensen, and J. A. Tullis, "Empirical versus model-based atmospheric correction of digital airborne imaging spectrometer hyperspectral data," *Geocarto Int.*, vol. 20, no. 4, pp. 21–28, 2005.

[19] H. K. Zhang *et al.*, "Characterization of Sentinel-2A and Landsat-8 top of atmosphere, surface, and nadir BRDF adjusted reflectance and NDVI differences," *Remote Sens. Environ.*, vol. 215, no. October 2017, pp. 482–494, 2018, doi: 10.1016/j.rse.2018.04.031.